PERGAMON

International Journal of Heat and Mass Transfer 46 (2003) 37–43

International Journal of HEAT and MASS TRANSFER

www.elsevier.com/locate/ijhmt

Molecular dynamics calculation of heat dissipation during sliding friction

B. Li [a,b,*], P.C. Clapp [a], J.A. Rifkin [a], X.M. Zhang [b]

[a] *Department of Metallurgy and Materials Engineering, University of Connecticut, 97 North Eagleville Road, Storrs, CT 06269-3136, USA*

[b] *Institute of Metal Research, Chinese Academy of Sciences, 72 Wenhua Road, Shenyang 110015, China*

Received 17 December 2001; received in revised form 30 June 2002

Abstract

A novel method of calculation of heat dissipation during sliding between metals was presented by using molecular dynamics. Temperature distribution in the regions near the contact interface was calculated. The calculation results show that plastic deformation in the near-surface regions accounts for most of the friction heat and the temperature increase. Friction heat was built up in the regions subject to plastic deformation. In the case that no plastic deformation occurred, elastic waves contributed mainly to the energy dissipation so that no large heat buildup could take place in the vicinity of the contact regions.

Keywords: Molecular dynamics; Friction; Heat dissipation

1. Introduction

Friction is a process involving very complicated energy dissipation, heat is produced at the frictional interface and energy is dissipated during friction. However, the mechanisms responsible for energy dissipation during friction are quite baffling, partly due to the difficulties in experimentation. Various models concerning friction have been proposed by a number of scientists and probably the most widely accepted is adhesion theory by Bowden and Tabor [1]. The adhesion theory demonstrates that when two metal surfaces are placed into contact, junctions are to be formed at the tips of the asperities, as a result of local plastic deformation. Consequently, work needs to be done to overcome the adhesion force in order to shear the junctions apart. Bowden and Tabor also included a plowing term to account for the energy dissipation. The adhesion theory focuses on the junctions formed between asperities due to adhesion, while other theories have made a lot of effort taking the plastic deformation occurring in the material at a considerable depth from the interface into consideration and a number of models were proposed [2,3], taking plastic deformation as a major source of dissipation. Macroscopic thermal models for sliding contact were proposed by a number of workers [4–9] in order to calculate the temperature distribution near the contacting surfaces. Plastic deformation models for sliding contact achieved good agreement between theories and experiments in some cases. However, these calculations involved various assumptions to simplify mathematics. The complexity makes the calculation of heat dissipation very difficult, and practically it is extremely difficult to determine the temperature distribution and temperature evolution in a mechanical system in which friction is taking place.

Molecular dynamics has long been applied to the study of friction phenomena, the simulation results present a view of frictional processes on an atomic scale

* Corresponding author. Address: Department of Metallurgy and Materials Engineering, University of Connecticut, 97 North Eagleville Road, Storrs, CT 06269-3136, USA. Tel.: +1-860-486-2784; fax: +1-860-486-4745.

E-mail address: binli@engr.uconn.edu (B. Li).

0017-9310/03/$ - see front matter
PII: S0017-9310(02)00258-2

Nomenclature

E	energy (J)
E_k	kinetic energy (J)
F	embedding energy (J)
k_B	Boltzmann constant ($J K^{-1}$ molecule^{-1})
m	mass of an atom (kg)
n	number of atoms
r	distance between atoms (m)
T	temperature (K)
v	velocity ($m s^{-1}$)
Φ	pair potential (J)
ρ	electron density (m^{-3})
Subscripts	
c.m	center of mass
i, j, k	atom indices
t	type of atom

or nanoscale [10–13]. So far the simulations have been mainly concentrated on the frictional dynamics such as stick-slip and interfacial behavior. In this work, molecular dynamics calculations of the temperature distribution both in the sliding block and substrate are presented. By performing these calculations, the mechanisms of energy dissipation can be identified, and the results obtained may offer a better understanding on the heat dissipation during sliding friction.

2. MD calculations of temperature distribution

2.1. Interatomic potential for Ni–Al alloy

The embedded atom method (EAM) was proposed by Baskes and co-workers [14,15] in 1983. In the EAM, the energy of a system can be expressed as the summation of a pairwise potential and an embedding energy that is a function of the local electron density. For binary systems, the energy expression for atom i is

$$E_i = \frac{1}{2}\sum_{j(\neq i)} \Phi_{t_i t_j}(r_{ij}) + F_{t_i}(\rho_i) \tag{1}$$

Here t_i and t_j indicate the elemental types of atoms i and j respectively, r_{ij} is the scalar distance between atoms i and j, Φ is a pairwise interaction potential, and ρ_i is the density at atomic site i due to all its neighbors,

$$\rho_i = \sum_{j(\neq i)} \rho_{t_j}(r_{ij}) \tag{2}$$

The embedding energy, $F(\rho_i)$ can be interpreted as the energy arising from embedding atom i in an electron gas of density ρ_i.

Using the EAM, Voter and Chen developed an EAM interatomic potential for the Ni–Al system [16,17]. In their model, the pairwise potential was taken to be a Morse potential, and the density of a hydrogen 4s orbital was used for the electron density function. This potential was slightly modified by Farkas et al. [18] because of its inaccuracy in describing stoichiometric B2 NiAl. This interatomic potential has been proved valid in a number of MD simulations [16,17,19]. By using this potential we have the flexibility of studying multiple combinations of members of tribocouples by just using one potential, for example Ni–Ni, Al–Al, Ni–Al, NiAl–NiAl etc., so that we can possibly investigate tribosystems with hardness difference existing in members of tribocouple.

2.2. Calculation method

Unlike other numerical methods, molecular dynamics simulations examine the motion of a collection of atoms based on their interactions. The energy of the system is exclusively determined by the interatomic potential. Once a system to be simulated is defined, i.e., system size (how many atoms are contained), boundary conditions (repeated boundary or free surface) and initial velocities (normally comply with a Maxwell–Boltzmann distribution at the desired temperature), no further assumptions are needed. Since the coordinates and the velocities of each particle can be computed and recorded at any time step during molecular dynamics simulations, the instantaneous kinetic energy of each atom at that particular time step can unambiguously be determined based on these data and the temperature distribution during frictional processes can be mapped on an atomic scale or nanoscale. However, the kinetic energy of each atom does not directly yield the instantaneous temperature, because there is a distribution for the velocities of the atoms in the system and the temperature distribution should be averaged over a certain range of atoms, which indicates that filtering algorithm should be used in the computation. On the other hand, the contribution from the sliding motion to the kinetic energy should be deducted when calculating the instantaneous temperature of each atomic site in the lattice space. More rigorously, the contribution from the angular motion of particles should also be taken into consideration, which is normally neglected in MD simulations. The instantaneous temperature of each site at a certain timestep is taken as the mean temperature over a neighborhood of atoms enclosed by a sphere of a radius r. The calculation procedure is as follows.

First, the total kinetic energy $(E_k)_{tot}$ of all the atoms in the sphere was calculated by summing over the kinetic energy of each atom:

$$(E_k)_{tot} = \frac{1}{2}\sum m_i(v_{ix}^2 + v_{iy}^2 + v_{iz}^2) \quad (3)$$

then the kinetic energy of the atom in the center of the sphere was given by

$$(E_k)_j = \frac{1}{n}[(E_k)_{tot} - (E_k)_{c.m}] \quad (4)$$

where n is the total number of the atoms in the sphere, j is referred to the jth atom in the system. The second term in Eq. (4) is the kinetic energy of the center of mass in the sphere:

$$(E_k)_{c.m} = \frac{1}{2}\sum m_i(\bar{v}_x^2 + \bar{v}_y^2 + \bar{v}_z^2) \quad (5)$$

and

$$\bar{v}_x = \frac{1}{k}\sum v_{ix} \quad \bar{v}_y = \frac{1}{k}\sum v_{iy} \quad \text{and} \quad \bar{v}_z = \frac{1}{k}\sum v_{iz} \quad (6)$$

where k is the number of the atoms which have a sliding velocity.

Second, the instantaneous temperature of each atomic site can be computed by

$$T_j = \frac{2(E_k)_j}{3k_B} \quad (7)$$

where k_B is the Boltzmann constant.

The filter size r has a little effect on the calculated temperatures. Larger filter produces lower temperatures, but the temperature distribution would be smoother. In this work, the filter size r was taken as 0.6 nm, which is empirical and covers up to the sixth nearest neighbors for NiAl alloy.

After the temperature of each atomic site in the system was calculated, color labels or grayscales were used to display the atoms according to their temperature range, for instance, red represents the highest temperature and yellow the second highest temperature, etc.

For all the simulations in this work, no external normal load was applied to the sliding block. In molecular dynamic simulations, the contact between the frictional surfaces is perfect and the interaction between surface atoms could be as strong as the bulk atoms, even stronger. This makes the formation and behavior of nanoscale junctions quite different from those of microscale junctions [20]. Adhesion in the nanoscale has significant effects in these situations. On the one hand, the overall adhesion force between the contact surfaces will enhance the normal force that the block exerts on the substrate. The adhesion force may be much more important than the contribution to the normal force. On the other hand, the adhesion effect between the two surfaces makes atomic-sized contact impossible, even though no external load was applied. The adhesion force tends to increase the contact area such that the nanoscale junctions rather than atomic-sized junctions will be formed.

2.3. Calculation results

2.3.1. Temperature distribution when sliding Ni on Al

The tribocouple was shown in Fig. 1. The substrate box comprised $60 \times 15 \times 8$ unit lattice cells or 28,800 Al atoms. The three dimensions were in X-[1 0 0], Y-[0 1 0] and Z-[0 0 1] directions. The upper block was composed

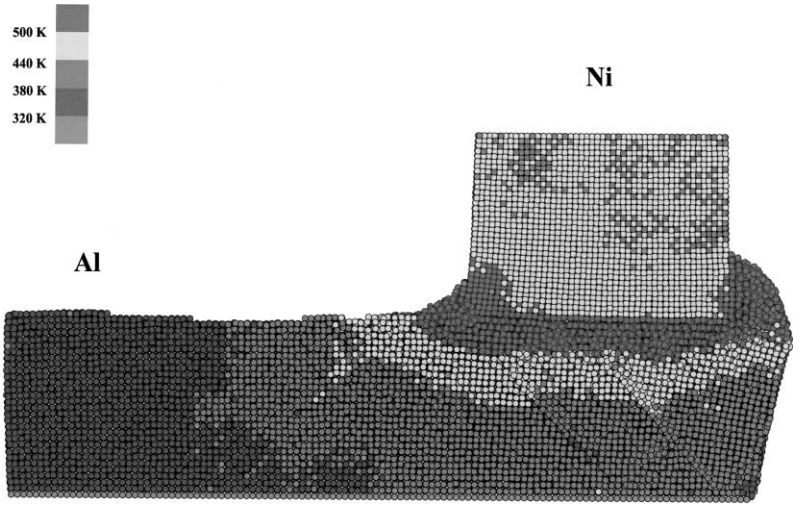

Fig. 1. Temperature distribution when sliding pure Ni on Al. Timestep: 23,000; velocity: 289 m s^{-1}; $F = 5.0 \times 10^{-6}$ dyn; upper block: 14,382 atoms, [1 0 0], [0 1 0] and [0 0 1]; lower block: 28,800 atoms, [1 0 0], [0 1 0] and [0 0 1]; starting temperature: 300 K.

of 14,382 Ni atoms, taking the same crystal orientations as the substrate. A constant external force $F = 5.0 \times 10^{-6}$ dyn was imposed on each of 567 atoms contained in a small box located in the center of the upper block in order to obtain a sliding velocity, and the direction of the force was along the X-[1 0 0], namely the upper block is moving from left to right in Fig. 1. To stop the substrate from moving along with the sliding block the bottom layer of Al atoms of the substrate were fixed at their original positions. This means that these atoms have zero kinetic energies during the simulation, but their potential energies are not equal to zero. Adiabatic thermal conditions were imposed on this tribosystem, meaning that no energy exchange can occur between the tribosystem and the environment, and the starting temperature is 300 K. Free surface boundary conditions were imposed in the [1 0 0] and [0 1 0] directions, but periodic boundary conditions were imposed in the [0 0 1] direction. The time step size in all the simulations was chosen as 2.5×10^{-15} s. This timestep size is empirical

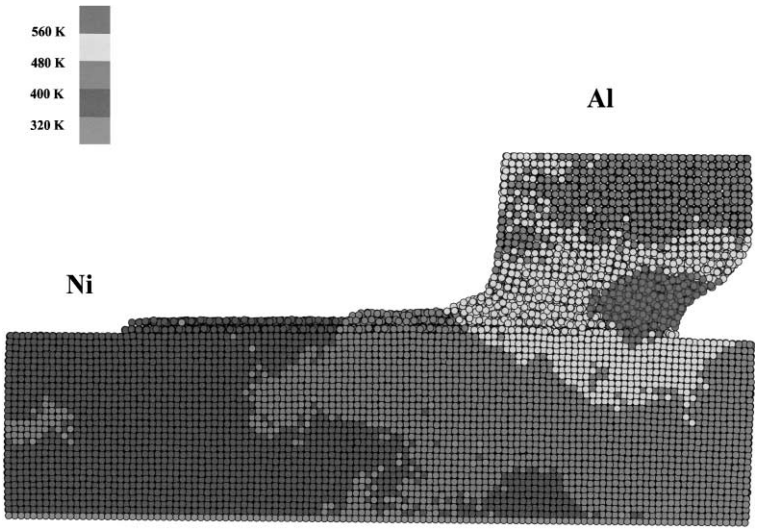

Fig. 2. Temperature distribution when sliding pure Al on Ni. Timestep: 25,000; velocity: 228 m s^{-1}; $F = 5.0 \times 10^{-6}$ dyn; upper block: 6370 atoms, [1 0 0], [0 1 0] and [0 0 1]; lower block: 28,800 atoms [1 0 0], [0 1 0] and [0 0 1]; starting temperature: 300 K.

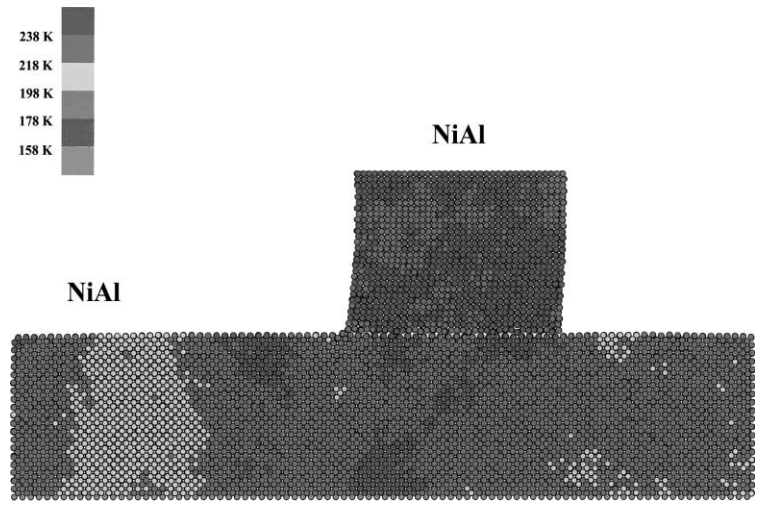

Fig. 3. Temperature distribution when sliding NiAl on NiAl. Timestep: 60,000; velocity: 50 m s^{-1}; $F = 5.0 \times 10^{-6}$ dyn; upper block: 5040 atoms, [1 1 0], [1 $\bar{1}$ 0] and [0 0 1]; lower block: 18,000 atoms, [1 0 0], [0 1 0] and [0 0 1]; starting temperature: 150 K.

and proved to be efficient in our simulations, under which the integral algorithm remained stable.

The temperature distribution at timestep 23,000 (57.5 ps after sliding began) when a pure Ni block slid on an Al substrate was shown in Fig. 1. From the color pattern it can be seen clearly that a thin layer of Al right underneath the contacting surfaces has the highest temperature increase. So does the pile-up in front of the shoveling edge of the Ni block.

2.3.2. Temperature distribution when sliding Al on Ni

The configuration is shown in Fig. 2, which is basically the same as the case of pure Ni on Al (Fig. 1). The Ni substrate comprises 28,800 Ni atoms and the upper block consists of 6370 Al atoms. A constant external force $F = 5.0 \times 10^{-6}$ dyn was imposed on each of 245 central group of atoms of the upper block. The starting temperature is 300 K.

As we can see from Fig. 2, a non-uniform pattern of temperature distribution was revealed in this case of pure Al sliding on a Ni substrate. The near-surface regions both in the upper block and the substrate heated up during the friction. Interestingly the hottest zone appeared in the vicinity of the front edge of the sliding block. A Similar distribution pattern was obtained when a higher external force was applied.

2.3.3. Temperature distribution when sliding NiAl on NiAl

Two different cases were studied when NiAl was slid on NiAl, as shown in Figs. 3 and 4, in which different external forces were imposed on the sliding block. Disorientation was set up for the sliding block and the substrate in order to prevent "cold weld". The substrate was in X-[1 0 0], Y-[0 1 0] and Z-[0 0 1], and the upper block was in X-[1 1 0], Y-[1 $\bar{1}$ 0] and Z-[0 0 1] directions. In the case of a lower driving force ($F = 5.0 \times 10^{-6}$ dyn) and a lower starting temperature (150 K), as shown Fig. 3, the sliding proceeded steadily and no wear took place at the interface. The temperature of the tribosystem looks uniformly distributed. In this case, pink rather than yellow was used to represent the second highest temperature. As we can see, there is no big temperature difference between the interface and the near-surface regions. Fig. 4 shows that the temperature distribution when a larger external force ($F = 1.0 \times 10^{-5}$ dyn) was applied. In this case a monolayer was peeled off and attached to the contacting surface and atom debris was accommodated between the two blocks and the interface became disordered. An amorphous tail was formed at the rear edge of the sliding block and exerted a strong resistance to the sliding. It can be seen from this pattern that the amorphous tail and its neighboring regions have the highest temperature.

2.3.4. Temperature distribution when sliding Al on Al

Fig. 5 shows the temperature distribution when a pure Al block was slid on an Al substrate. The sliding block is in the [1 0 0], [0 1 0] and [0 0 1] directions, containing 5800 atoms, and the substrate is in the [1 1 0], [$\bar{1}$ 1 1] and [1 $\bar{1}$ $\bar{2}$] directions, comprising 23,608 atoms. An external force $F = 2.0 \times 10^{-6}$ dyn was applied on the central group of atoms of the sliding block. Similar temperature distribution pattern was observed, a layer of Al atoms were pulled off and adhered to the substrate, the hottest region appears at the rear edge of the upper block, where an amorphous tail was formed.

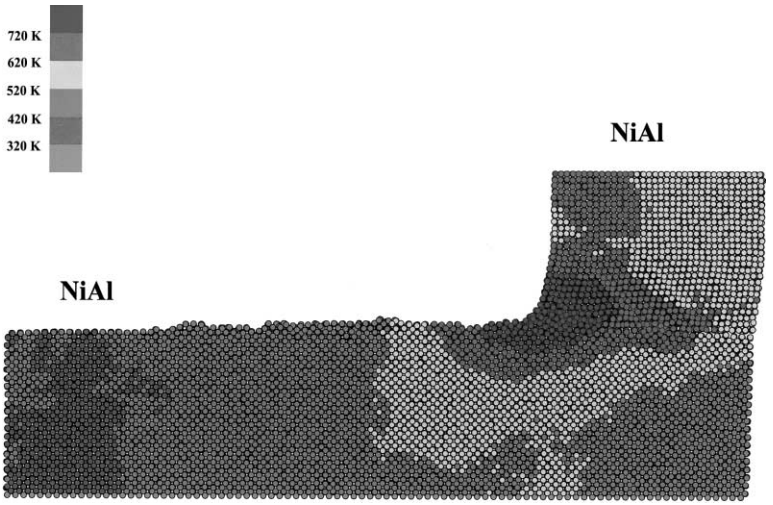

Fig. 4. Temperature distribution when sliding NiAl on NiAl. Timestep: 27,000; velocity: 273 m s^{-1}; $F = 1.0 \times 10^{-5}$ dyn; upper block: 5040 atoms, [1 1 0], [1 $\bar{1}$ 0] and [0 0 1]; lower block: 18,000 atoms, [1 0 0], [0 1 0] and [0 0 1]; starting temperature: 300 K.

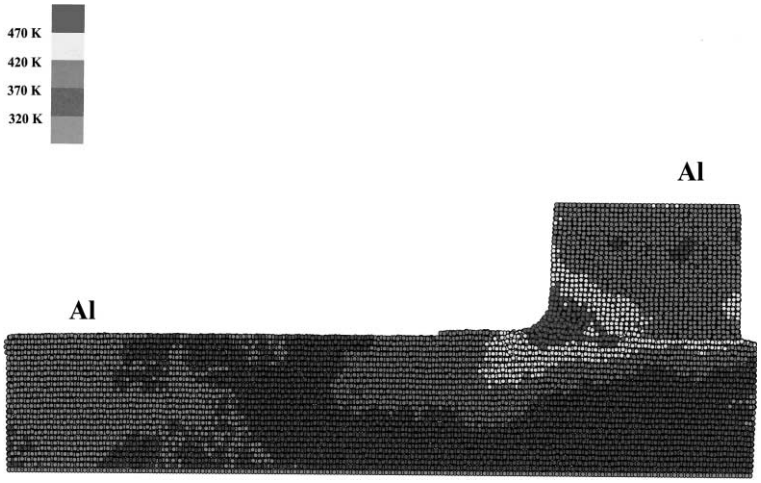

Fig. 5. Temperature distribution when sliding pure Al on Al. Timestep: 26,000; velocity: 265 m s^{-1}; $F = 2.0 \times 10^{-6}$ dyn; upper block: 5800 atoms, [1 0 0], [0 1 0] and [0 0 1]; lower block: 23,608 atoms, [1 1 0], [1 $\bar{1}$ 1] and [1 $\bar{1}$ $\bar{2}$]; starting temperature: 300 K.

3. Analyses and discussion

The calculation results in this work are interesting and revealing. The temperature distribution patterns in all the simulated tribosystems clearly indicate that plastic deformation near the contacting surface plays a major role in the energy dissipation during friction.

In the case that a pure Ni block was moving on an Al substrate (Fig. 1), a typical "plowing" process was observed. At the front edge of the upper block, Al atoms were shoveled and piled up against the edge. Shoveling occurred because a layer of Al atoms closest to the contacting Ni surface were peeled off and stuck to the Ni surface, due to the fact that the interaction between Ni–Al is much stronger than that between Ni–Ni and Al–Al. During the sliding the attached monolayer of Al atoms were carried along with the upper block, acting as a shovel edge. As the sliding process continued, the density of dislocations increased in the substrate. The disordered regions in the substrate expanded, and an apparent dislocation slip band at an angle of 45° with the interface can be clearly seen. This means plastic flow was now occurring.

From Fig. 1 we can clearly see, that heat was built up in a thin layer of Al underneath the interface and also in the bulge formed in front of the sliding block, because the material of these regions was very highly deformed. Under the strong action of shear force breaking down the adhesive bonds, even amorphisation could occur locally.

In the case of pure Al sliding on a Ni substrate, the hottest region appears near the front edge of the sliding block, because a strong plastic flow is going on in this region. As shown in Fig. 2, two layers of Al atoms were left behind and attached themselves to the Ni surface while the Al block was sliding forward under the action of the external force. This coating layer steadily grew as the sliding continued. It also can be seen in Fig. 2 that the front edge of the upper block was being consumed by the transfer of material of this region to the substrate.

Similar distribution patterns were obtained in the cases that NiAl was slid on NiAl (Fig. 4) and pure Al on Al (Fig. 5), though the hottest zones came up in the rear edge of the sliding blocks. These regions were also subject to severe plastic deformation or plastic flow.

The two cases of NiAl on NiAl (Figs. 3 and 4) provide a good comparison showing what happens to energy dissipation when plastic deformation is present or absent in the near-surface region. In the case (Fig. 3) in which no plastic deformation took place (but obviously lattice elastic deformation occurred near the interface), there is no significant heat buildup at the interface, and the temperature is fairly well distributed. In all the cases in which plastic deformation took place in the near-surface regions, heat was built up in these regions, therefore, the local plastic deformations accounted for most of the energy dissipation. As we can see from these results (Figs. 4 and 5), the plastic deformations taking place in the near-surface regions exert strong resistance to the sliding motion of the upper block, the plastic work is dissipated as friction heat.

Generally a frictional force can be produced by storing or dissipating energy in a number of ways. Rigney and Herth [5] enumerates the following possible energy dissipation processes: anelastic or elastic deformations, phase transformations and other structural changes, plastic deformations. And, plastic deformation was considered as the major contribution to friction. In our simulations, no phase transformation in large scale occurred within the sliding block and the substrate, except that disordering did happen near the interface,

which was due to the co-action of the adhesion and the shear force. In some experiments in which the QCM was used to determine energy dissipation during friction, those results show that all of the friction was attributed to phonons [21]. This is because in the QCM experiments the friction is purely interfacial and wear-free. In the slower slider case in Fig. 3, the sliding process was wear-free, and the friction work was transformed into the kinetic and potential energy of the system, this must have happened via elastic waves which were generated and released at the interface. In our simulations, an interesting oscillation in the potential energy of the substrates was also observed in the cases in which one member of the tribocouple was pure Al, or both blocks were Al (Fig. 1, Figs. 2 and 5). This type of oscillations in potential was also observed in other MD simulations of friction [11–13]. It indicates that elastic waves were propagating in the substrates. Calculations performed in our work [22] show that the energy oscillations mainly come from those atoms located in the contact regions. This is evident that a sound wave was being generated at the interface and traveling through the substrate, as a result of the breakdown of the adhesive bonds. As we can see from the temperature distribution profiles, phonons are almost certainly not responsible for the local heat buildup. In all the faster slider cases, phonons maybe take up a relatively smaller part of the energy dissipation, compared with the plastic deformation, which is the major source of heat dissipation.

4. Conclusions

The molecular dynamics calculations of the temperature distribution during sliding friction show that plastic deformation in the near-surface regions accounts for most of the friction heat and the temperature increase. Friction heat was built up in the regions subject to plastic deformation. In the case that no plastic deformation occurred, elastic waves contributed mainly to the energy dissipation so that no large heat buildup could take place in the vicinity of the contact regions.

References

[1] F.P. Bowden, D. Tabor, The Friction and Lubrication of Solids, The Clarendon Press, Oxford, England, 1954, p. 300.
[2] N.P. Suh, P. Sridharan, Wear 34 (1975) 291–299.
[3] D. Walton, J. Appl. Phys. 33 (1962) 519–526.
[4] N.R. DesRuisseaux, R.D. Zerkle, J. Heat Transfer 92 (1970) 456–464.
[5] D.A. Rigney, J.P. Hirth, Wear 53 (1979) 345–370.
[6] A.D. Dimarogonas, Wear 23 (1973) 113–119.
[7] F.R. Berry, J.R. Barber, The division of fictional heat—a guide to the nature of sliding contact, J. Tribol., ASME 106 (1984) 405–415.
[8] M. Rashid, A. Seireg, Heat partition and transient temperature distribution in layered concentrated contacts, J. Tribol., ASME 109 (1987) 496–502.
[9] P. Chantrenne, M. Raynaud, Int. J. Heat Mass Transfer 40 (1997) 1083–1094.
[10] U. Landman, W.D. Luedtke, E.M. Ringer, Wear 153 (1992) 3–30.
[11] J.A. Nieminen, A.P. Sutton, J.B. Pethica, Static junction growth during friction sliding of metals, Acta Metall. Mater. 40 (1992) 2503–2509.
[12] J.A. Harrison, C.T. White, R.J. Colton, D.W. Brenner, Phys. Rev. B 46 (1992) 9700–9708.
[13] M.R. Sorensen, K.W. Jacobsen, P. Stoltze, Phys. Rev. B 53 (1996) 2101–2113.
[14] M.S. Daw, M.I. Baskes, Semiempirical, quantum mechanical calculation of hydrogen embrittlement in metals, Phys. Rev. Lett. 50 (1983) 1285–1288.
[15] M.S. Daw, M.I. Baskes, Phys. Rev. B 29 (1984) 6443–6453.
[16] A.F. Voter, S.P. Chen, MRS Symp. Proc. 82 (1987) 175.
[17] S.P. Chen, D.J. Srolovitz, A.F. Voter, J. Mater. Res. 4 (1989) 62–77.
[18] D. Farkas, B. Mutasa, C. Vailhe, K. Ternes, Model. Simul. Mater. Sci. Eng. 3 (1995) 201–207.
[19] Y. Shao, P.C. Clapp, J.A. Rifkin, Metall. Mater. Trans. A 27A (1996) 1477–1489.
[20] N.J. Persson, in: Sliding Friction: Physical Principles and Applications, Springer, Berlin, New York, 1998, p. 57.
[21] M.O. Robins, J. Krim, MRS Bull. (1998) 23–26.
[22] B. Li, P.C. Clapp, J.A. Rifkin, X.M. Zhang, J. Appl. Phys. 9 (2001) 3090–3094.